AIP | Journal of Applied Physics

Platinum enhanced textured growth of grainaligned YBa2Cu3O7−x thick films

M. R. Wegmann, J. A. Lewis, and C. E. Platt

Citation: J. Appl. Phys. **75**, 5218 (1994); doi: 10.1063/1.355719
View online: http://dx.doi.org/10.1063/1.355719
View Table of Contents: http://jap.aip.org/resource/1/JAPIAU/v75/i10
Published by the American Institute of Physics.

Platinum enhanced textured growth of grain-aligned $YBa_2Cu_3O_{7-x}$ thick films

M. R. Wegmann and J. A. Lewis
Science and Technology Center for Superconductivity, and the Department of Materials Science and Engineering, University of Illinois at Urbana-Champaign, Urbana, Illinois 61801

C. E. Platt
Science and Technology Center for Superconductivity, University of Illinois at Urbana-Champaign, Urbana, Illinois 61801

(Received 10 November 1993; accepted for publication 3 February 1994)

The effects of magnetic alignment, heat treatment, and substrate interactions on the microstructural development and properties of $YBa_2Cu_3O_{7-x}$ (Y123) thick films were studied. Aligned films were formed by vacuum filtrating a particulate suspension in a 7 T applied field. These films and nonaligned control films were fired on either platinum (Pt) foil or magnesium oxide (MgO) substrates to various maximum temperatures between 930 and 1040 °C. Optical microscopy revealed large differences in microstructural development between the various films. Aligned Y123 films fired on Pt foil exhibited the best microstructural properties. Via plasma emission spectroscopy and secondary ion mass spectroscopy, approximately 0.1 wt % Pt was found distributed throughout the films fired on platinum, while negligible amounts of Mg were detected in the films fired on MgO substrates. Differential thermal analysis revealed that, in the presence of Pt, the peritectic temperature (1030 °C for pure Y123 in O_2) is reduced 70 °C, thereby opening a substantial thermal processing window for partial melt assisted growth of textured Y123. SQUID measurements of magnetic hysteresis and T_c provided quantitative evidence that, relative to the films fired on MgO, those fired on Pt exhibited enhanced texture development [$\Delta M(H_{app}\|c \text{ axis})/\Delta M(H_{app}\perp c \text{ axis})=2.6$ at 5 K, 1 T] and properties (Bean model $J_{c,m}=5\times10^4$ A/cm^2 at 5 K, 4 T) without degradation of the T_c characteristics.

I. INTRODUCTION

$YBa_2Cu_3O_{7-x}$ (Y123) remains a viable material for further research due to its low thermal flux creep, relatively low toxicity, and ready availability of commercial precursors and powders. The goal is to process polycrystalline material with superconducting properties approaching those of well-pinned single crystals. However, bulk transport properties are degraded by weak link behavior stemming from a number of possible sources, including high angle grain boundaries, insulating impurity layers, residual porosity, and microcracks.[1–4] Solving these problems has spawned a wealth of research into new fabrication methods and process additives.

A technique aimed at improving the superconducting properties of bulk Y123 is melt processing. During this process, a liquid is formed as Y123 decomposes incongruently (Y123−>Y211+liquid) upon heating above the peritectic temperature T_p of 1030 °C in pure O_2(g). The presence of the liquid phase is beneficial because it promotes the dissolution of impurities, enhances the grain growth rate, and leads to high final densities without an applied external pressure. Besides these general advantages of melt processing, melt texturing of Y123[4–8] capitalizes on the tenfold larger current carrying capacity in the *a-b* plane than along the *c* axis.[9] Melt texturing has been achieved either by the melt-quench-melt-growth (MQMG) method,[4–6] or by directional solidification.[7,8] However, both approaches have their limitations. In MQMG processing, large textured Y123 domains form upon recrystallization, but these are poorly aligned within the bulk of the sample. This problem is addressed in directional solidification which produces highly oriented bulk material, but only at extremely slow growth rates (≈1 μm/s), as shown by Cima *et al.*[8]

Grain aligned Y123 can also be produced via processing in an applied magnetic field by exploiting the normal state anisotropic paramagnetic susceptibility which promotes alignment of Y123 crystallites with their *c* axis parallel to the applied field.[10] A common approach is to fabricate films of Y123 powder in an applied field followed by solid state densification in zero field.[11–13] An alternative method is to densify the material in an applied field, either below[14] or above[15] the peritectic temperature. The former two methods result in a well aligned, but weakly linked fine grained material. In contrast, melt processing in an applied field produces oriented material with greatly enhanced properties. However, *in situ* thermal processing in an applied magnetic field is technologically complex.

Chemical additions to Y123 have also been studied to determine their effects on processing and properties.[16–19] Specifically, platinum (Pt) doping in Y-Ba-Cu-O has been evaluated primarily to determine its influence on the microstructural development of the insulating Y_2BaCuO_5 (Y211) phase during melt processing. It has been proposed that Pt inhibits growth of the Y211 phase, resulting in a homogeneous dispersion of fine Y211 precipitates in the Y123 bulk and a significant improvement in superconducting properties compared to samples without Pt doping. Furthermore, it has been shown that suppression of the superconducting transition temperature T_c by additions of platinum into conven-

 0021-8979/94/75(10)/5218/9/$6.00

tionally sintered Y123 can be almost completely recovered by melt processing.[20]

We have previously demonstrated that textured Y123 thick films can be produced by vacuum filtration of particulate suspensions in an applied magnetic field at ambient conditions, followed by partial melting.[21] Here, we define partial melting as the incomplete transformation of Y123 to Y211 and the liquid phase during heat treatment. Thus, in this process unmelted aligned Y123 particles that serve as nucleation sites for textured growth upon recrystallization remain in the microstructure. This approach draws on the benefits of both magnetic alignment and melt processing while keeping them separate during film fabrication. We have also shown that platinum significantly suppresses the peritectic temperature of Y123.[22] In this article we have expanded our work to investigate the thermal processing conditions required to optimize the texture development and properties of partially melt processed bulk aligned Y123 in the presence of Pt. We have found that interactions with Pt lead to greatly enhanced microstructural development and improved properties compared to pure partially melt processed bulk aligned Y123.

II. EXPERIMENTAL PROCEDURE

A. Thick film processing

Thick films (disks≈1.0 mm thick, 20 mm in diameter) of Y123 were produced by vacuum filtrating a particulate suspension. The suspensions consisted of 78.0 wt % isopropyl alcohol, 21.4 wt % Y123 powder (2–6 μm),[23] and 0.6 wt % menhaden fish oil as a dispersant. A small amount of suspension in an appropriate sample holder was lowered into the room temperature vertical bore of a 7 T superconducting magnet[24] where the powder was allowed to align and settle out of suspension. The magnetic field was oriented perpendicular to the surface of the resulting film. The excess solvent was removed from the thick film by vacuum filtration, and then the applied field was removed. The films were allowed to dry at ambient temperature for several hours. The same procedure was performed in zero field to produce nonaligned control samples.

Films were fired according to the schedules presented in Fig. 1 in a controlled atmosphere tube furnace.[25] The initial ramps to 650 °C were performed under 100 cc/min flowing nitrogen and the remainder of the schedules under 100 cc/min flowing oxygen. Solid state sintering experiments were performed at 930 °C for 10 h. Partial melt processing experiments were conducted to maximum temperatures T_{max} of 1010, 1020, 1030, and 1040 °C. Each experiment contained four samples: two samples, one each aligned and nonaligned, on polycrystalline Pt substrates[26] (99.99% purity), and two samples, one each aligned and nonaligned, on MgO substrates[27] (cleaved 100 orientation).

B. Microstructural characterization

X-ray diffraction (XRD)[28] analysis was performed on the film surfaces of the as-cast and fired samples to give a quantitative measure of texture development. Portions of the fired films were ground to a fine powder with an agate mortar and pestle and analyzed for Pt and Mg using inductively coupled plasma emission spectroscopy (ICP).[29] Any reaction layer present at the interface between the sample and the substrate was removed prior to grinding. To characterize microstructural development and phase distribution in the films, optical microscopy with polarized light[30] and secondary ion mass spectroscopy (SIMS)[31] imaging were used on polished film cross sections. Isopropyl alcohol or kerosene were used as lubricants during rough grinding and oil-based diamond slurries were used for fine polishing to a 1 μm finish.

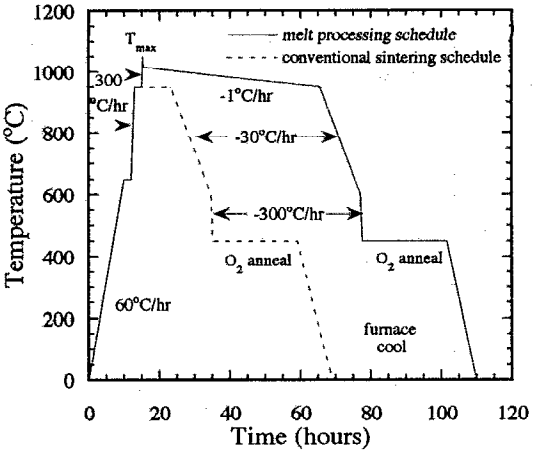

FIG. 1. Heat treatment schedules for Y123 thick films.

C. Magnetic measurements

Magnetic property measurements of the polycrystalline samples (approx. 2 mm×2 mm×0.5 mm) were performed using superconducting quantum interference device (SQUID) magnetometers.[32] Transition temperature measurements were performed on a low-field SQUID (1 T maximum field). Samples were zero field cooled to 60 K and ramped to 100 K in 1 or 2 K increments in an applied field H_{app} of 5 mT oriented perpendicular to the sample surface. Magnetization measurements were performed on a high-field SQUID (5.5 T maximum). Samples were oriented with the applied field either perpendicular to the sample surface ($H_{app} \| z$, where z is the film normal) or parallel to the surface ($H_{app} \perp z$). In the aligned films this corresponded to the applied field parallel to the c-axis texture ($H_{app} \| c$ axis) or perpendicular to the c-axis texture ($H_{app} \perp c$ axis), respectively. The samples were zero field cooled to 5 K and hysteresis measurements were taken from 0 to 5.5 T, from 5.5 to −5.5 T, and back to 5.5 T.

D. Differential thermal analysis

Y123 powder was mixed with either 1, 3, 5, or 10 wt % Pt powder[33] (0.8–2.2 μm) using an agate mortar and pestle. Similar mixtures were prepared with additions of MgO powder.[34] Samples of these mixtures and of pure Y123 without additions were heated at 5 °C/min to 1100 °C in 10 cc/min flowing oxygen in a differential thermal analyzer (DTA)[35] in alumina crucibles.

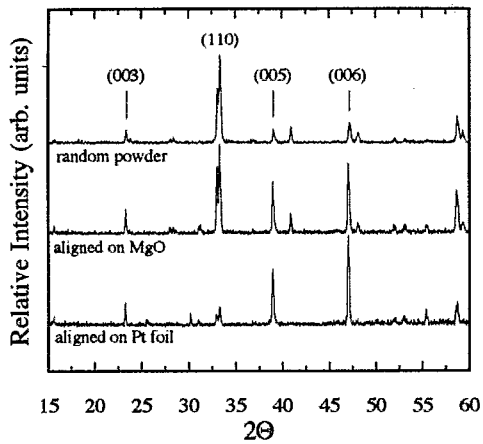

FIG. 2. XRD patterns for random Y123 powder and densified Y123 films fired to $T_{max}=1010$ °C on Pt foil and MgO substrates.

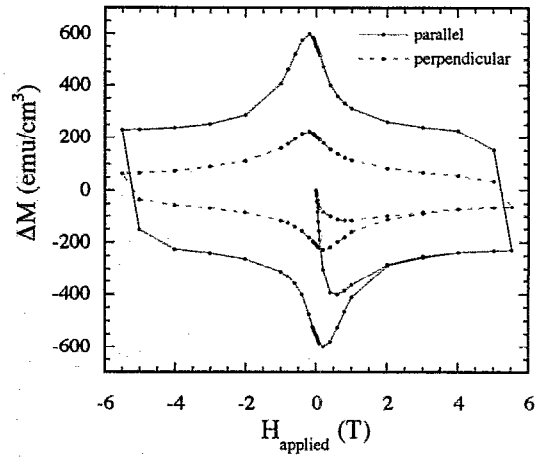

FIG. 4. Hysteresis loops at 5 K for $H_{app}\|c$ and $H_{app}\perp c$ for a Y123 thick film fired to 1010 °C on Pt foil.

III. RESULTS

A. Texture development

XRD analysis of the as-cast and of the fired films revealed a significant amount of texture in the aligned films, as shown in Fig. 2. Compared to the random powder pattern, the relative intensity (I) of the ($00l$) peaks representing the preferentially superconducting a-b planes is increased in the fired films, particularly for films densified on Pt foil. To quantify the degree of c-axis texture at the surface of a film, an orientation factor $P_{006}=1-\beta$, where $\beta=(I_{110}/I_{006})^{\text{aligned}}/(I_{110}/I_{006})^{\text{nonaligned}}$, was utilized. This factor compares the relative intensity of the (110) peak, the strongest reflection in the random powder pattern, to the relative intensity of the (006) peak. Thus, one expects a P_{006} value near zero in a randomly oriented film and a P_{006} value approaching 1.0 for a well c-axis textured film. P_{006} averaged to about 0.75 for the as-cast aligned films. The values of P_{006} calculated for the fired aligned films are summarized in Fig. 3. Here, the films fired on Pt generally exhibited better surface texture. For the films fired on MgO, no improvement in texture was observed between $T_{max}=930$ and 1010 °C, while the films fired on Pt showed a significant increase. Surface texture was maximized at 1010 °C on Pt and at 1020 °C on MgO. In both films heated to 1040 °C a precipitous drop in P_{006} was observed.

Bulk grain alignment was quantified by magnetization measurements. A representative pair of hysteresis loops are shown in Fig. 4. The anisotropy of the magnetization response for a given film was calculated as the ratio $R=\Delta M(H_{app}\|c \text{ axis})/\Delta M(H_{app}\perp c \text{ axis})$. A ratio on the order of 1.3 at 1 T was determined for the as-cast aligned films. For the fired films, R values calculated at 1 T are shown as a function of maximum firing temperature in Fig. 5. As was observed for the P_{006} results, no improvement in texture was found between $T_{max}=930$ and 1010 °C for the aligned films fired on MgO, but the aligned films fired on Pt showed a

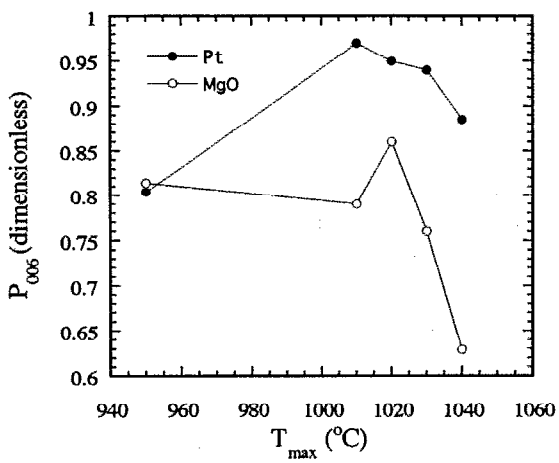

FIG. 3. Surface anisotropy of densified Y123 films as characterized by XRD, where the ratio P_{006} is shown as a function of maximum firing temperature.

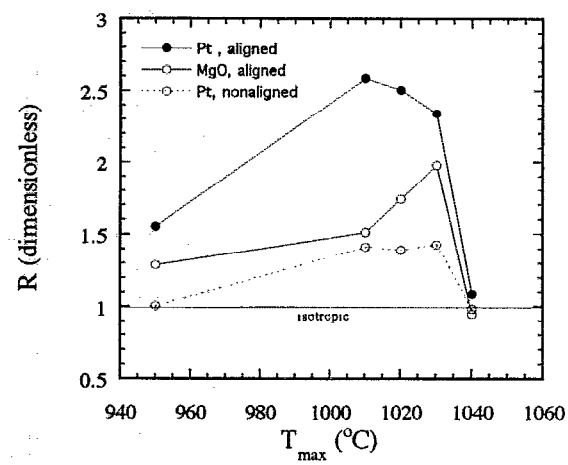

FIG. 5. Bulk anisotropy of densified Y123 films as characterized by SQUID, where the ratio $R=\Delta M(H_{app}\|c)/\Delta M(H_{app}\perp c)$ at 5 K, 1 T is shown as a function of maximum firing temperature.

significant increase in preferred orientation. The anisotropy was maximized at 1010 °C on Pt and at 1030 °C on MgO, and diminished considerably at 1040 °C in both cases. The equivalent nonaligned films fired on Pt displayed significantly less anisotropy at any given temperature.

Optical micrographs taken under polarized light of aligned films fired to a maximum temperature of 1030 °C on MgO and Pt substrates are shown in Figs. 6(a) and 6(b), respectively. The fine grained (1–50 μm), porous microstructure of the sample fired on MgO is characteristic of a conventionally sintered material. Similar microstructures were observed in the samples fired to 930, 1010, and 1020 °C on MgO and at 930 °C for samples fired on Pt. In contrast, the textured, large grained (100–200 μm) dense microstructure of the sample fired on Pt to 1030 °C is indicative of a melt processed material. Similar results were observed for the samples fired at 1010 and 1020 °C on Pt.

Figure 6(c) shows the optical micrograph of the unaligned film fired to a maximum temperature of 1030 °C on Pt. Comparison with its aligned counterpart in Fig. 6(b) reveals the significant impact of the magnetic alignment process. Clearly, the aligned sample exhibits a preferred orientation of its grains in the plane of the film not observed in the nonaligned film. Also, a much larger average grain size ($\approx$150 μm) was observed for the aligned films with respect to the nonaligned specimens ($\approx$30 μm).

Figures 7(a) and 7(b) show the microstructures of aligned samples fired on MgO and Pt, respectively, to T_{max}=1040 °C. In both cases very large grains (~1 mm) were observed and no indications of preferred orientation were visible. Similar characteristics were observed in the equivalent nonaligned samples.

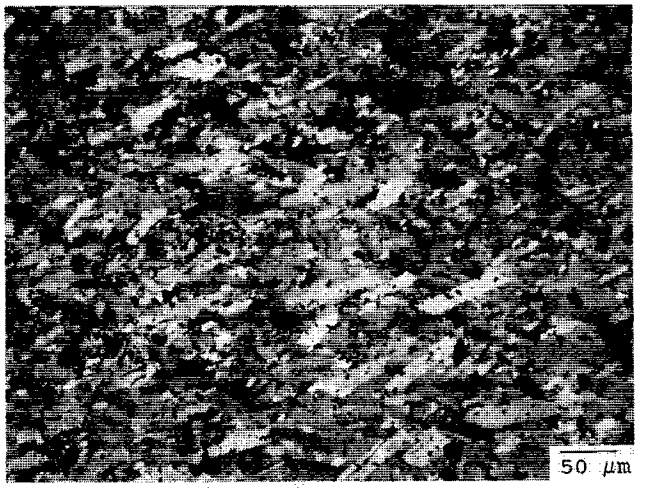

(a)

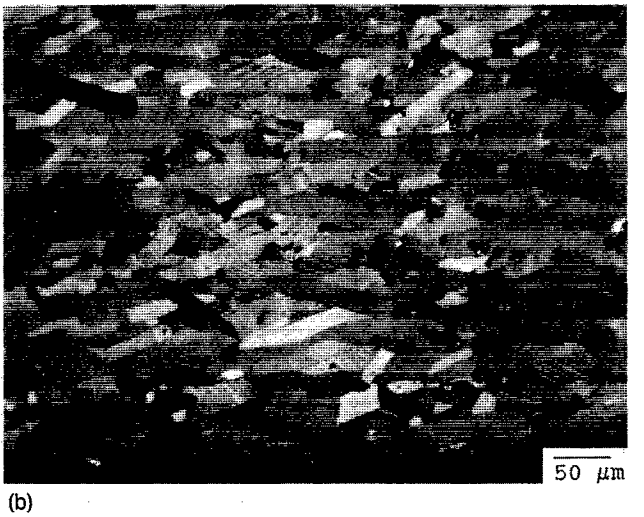

(b)

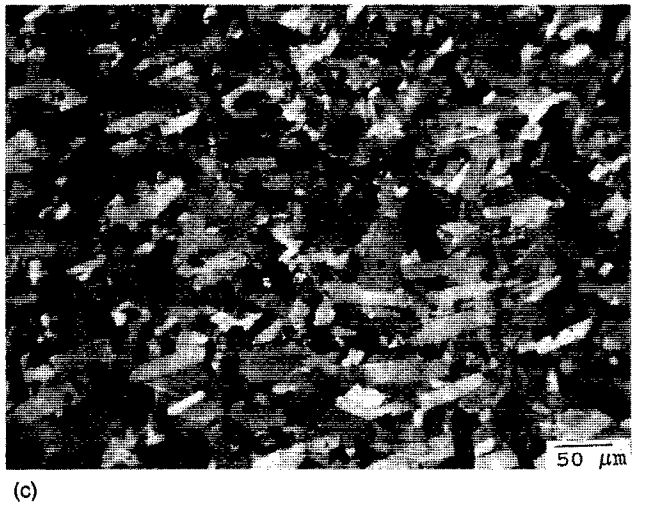

(c)

FIG. 6. Optical micrographs under polarized light of Y123 films fired to T_{max}=1030 °C: (a) aligned on MgO substrate; (b) aligned on Pt substrate; and (c) nonaligned on Pt substrate.

B. Film-substrate interactions

The purpose of the DTA analysis was to establish the mechanism leading to the disparate microstructural development between films fired on MgO and Pt. Figure 8 shows the DTA heating curves in the range 900–1100 °C of pure Y123 powder and of Y123 intimately mixed with varying concentrations of Pt and MgO powders. The absence of any extraneous peaks in the curve for the pure Y123 powder indicated that it was phase pure and that any reactions with the alumina crucible were negligible. A single, well-defined endothermic peak was observed near 1030 °C for pure Y123 that corresponds to the incongruent melting of this phase. With increasing Pt additions the results show clearly the development of an endothermic peak near 960 °C with a corresponding decrease in the pure Y123 endotherm at 1030 °C. No shift in the peritectic temperature was observed for the corresponding additions of MgO, for which only the 10 wt % data are shown here.

Table I shows a summary of the Pt and Mg content in the fired films as determined by ICP. The Mg concentration in the films fired on MgO was negligible up to a maximum firing temperature of 1040 °C, where a significant concentration increase was measured. In contrast, an average of 0.1 wt % Pt was incorporated into the films fired on Pt substrates above 930 °C.

A SIMS map of a region near the substrate in a film fired on Pt to 1030 °C is shown in Fig. 9(a). Comparison with the map for yttrium in Fig. 9(b) shows that Y-rich regions (Y211) were devoid of Pt. [Note that a schematic of the

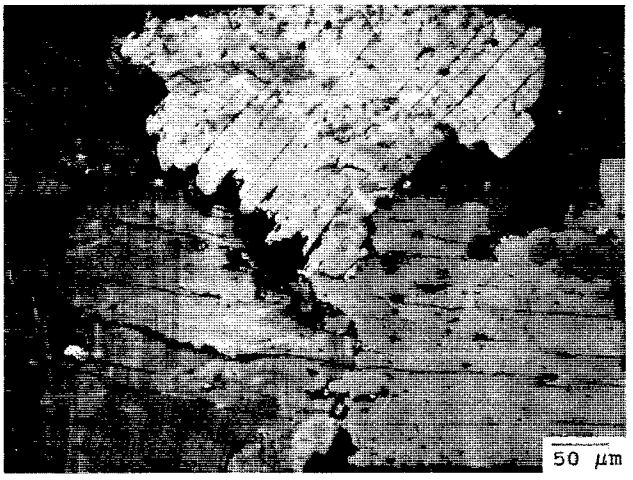

(a)

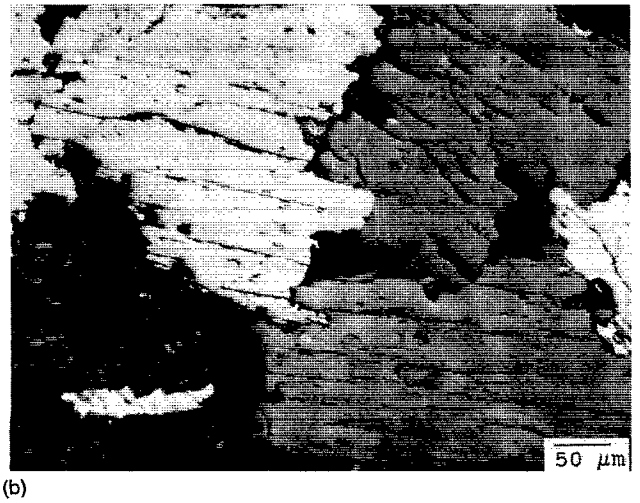

(b)

FIG. 7. Optical micrographs under polarized light of aligned Y123 films fired to $T_{max}=1040$ °C: (a) on MgO substrate and (b) on Pt substrate.

region is shown in Fig. 9(e) to help clarify the imaging data.] Comparison to the optical micrograph of a similar sample in Fig. 6(b) shows that the geometry of the regions with slightly higher Pt concentrations is similar to the grain boundary geometry. Comparison to Figs. 9(c) and 9(d), which are maps for barium and copper, respectively, show that Pt-rich regions were not exclusively Pt, but contained Y, Ba, and Cu. In mid-sample maps (not shown), however, the Pt concentration gradients were so small that the bulk distribution of Pt could be considered essentially homogeneous. Scanning electron microscopy (SEM) with energy dispersive spectroscopy (EDS) and backscattered electron (BSE) imaging largely corroborated these results.[36]

C. Superconducting properties

Magnetization T_c curves for the aligned Y123 samples fired on MgO and Pt substrates are shown in Figs. 10(a) and 10(b), respectively. Both displayed relatively broad transitions for the samples densified at 930 °C. These transitions became sharper at the intermediate maximum firing temperatures and broadened considerably for samples fired to

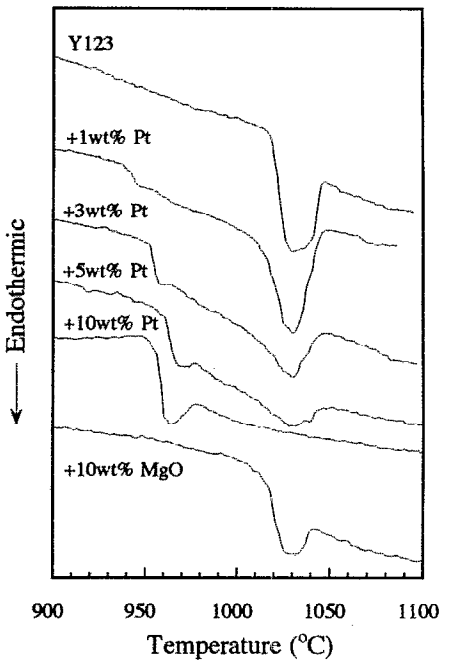

FIG. 8. DTA heating curves in oxygen of pure Y123 powder and Y123 powder mixed with varying concentrations of Pt and MgO.

1040 °C. All films showed transition onsets a few degrees below 90 K, with the exception of the film fired on MgO to 1040 °C, which showed a transition onset below 80 K. The high concentration of Mg in this film, as determined by ICP, suggests that the depressed transition temperature arises from Mg poisoning.

The magnetization hysteresis data is shown in Fig. 11, where ΔM ($H_{app} \| c$ axis) is plotted as a function of the applied magnetic field at 5 K. Figures 11(a) and 11(b) show that both films sintered conventionally at 930 °C on either MgO or Pt substrates, respectively, had poor flux pinning with increasing field and small magnetization responses at all fields. With increasing maximum firing temperature, films fired on MgO substrates exhibited a gradual improvement in pinning with a maximum ΔM of 3×10^2 emu/cm^3 at 5 T. In contrast, films fired on Pt to only 1010 °C exhibited strong pinning and ΔM values of 3×10^2 emu/cm^3 at 5 T, while increasing the maximum firing temperature above 1010 °C led to only modest improvements in the magnetization response.

The critical current density J_c was calculated from the magnetization hysteresis data by applying the Bean model

TABLE I. ICP results for fired Y123 films.

T_{max} (°C)	Y123 on Pt wt % Pt	Y123 on MgO wt % Mg
930	-	<0.01
1010	0.101	<0.01
1020	0.081	<0.01
1030	0.062	<0.01
1040	0.16	0.112

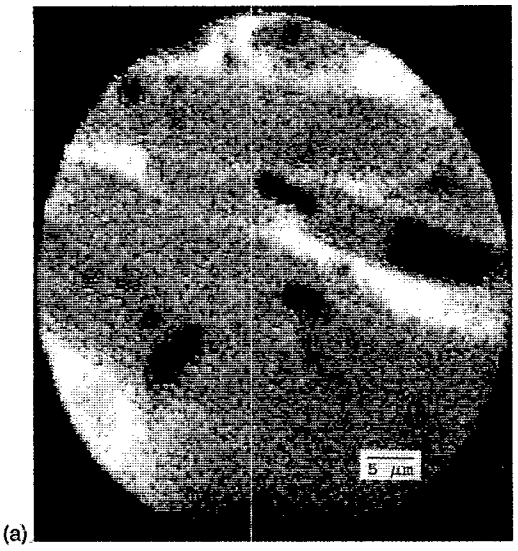

(a)

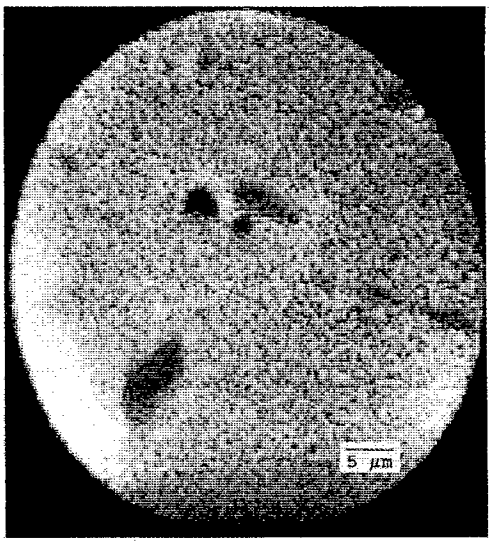

(d)

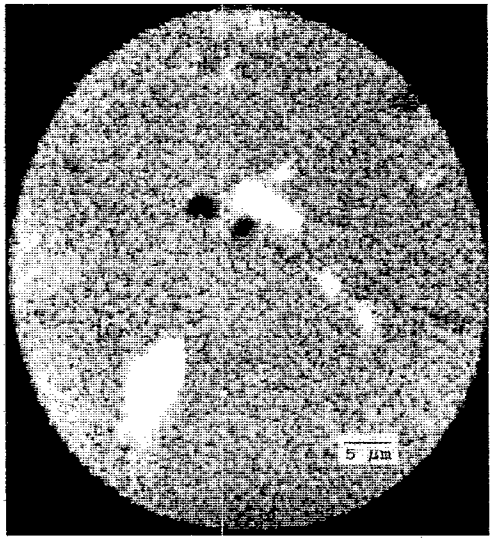

(b)

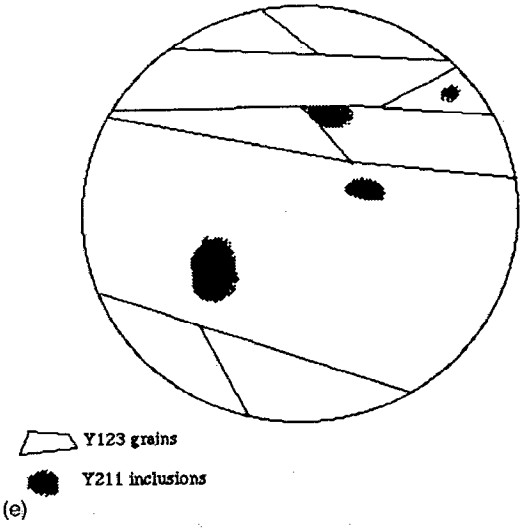

(e)

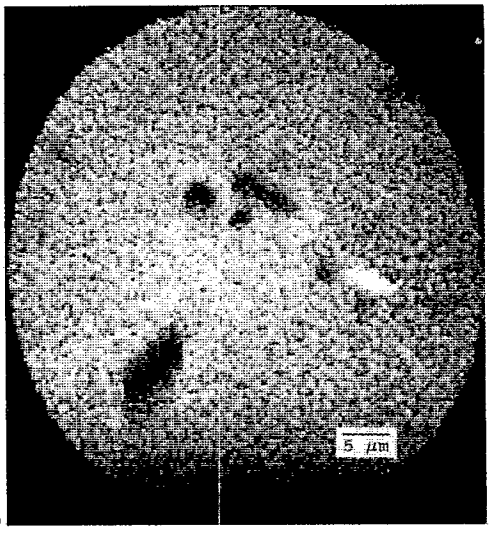

(c)

FIG. 9. SIMS maps for (a) platinum, (b) yttrium, (c) barium, and (d) copper of a Y123 film fired to $T_{max}=1030$ °C on Pt. (Note that brightness is proportional to the concentration of the element being mapped.) A schematic illustration of the region analyzed emphasizing the most important microstructural and compositional features is shown in (e).

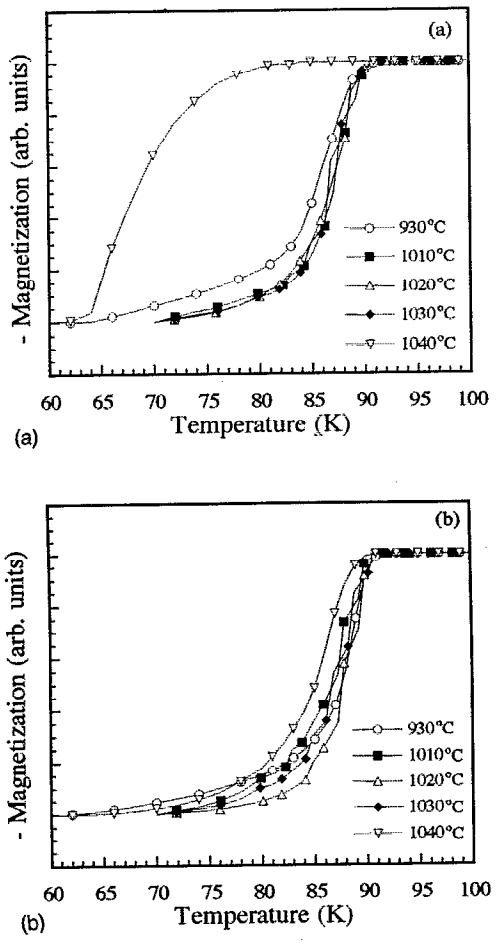

FIG. 10. Magnetization T_c curves for aligned Y123 films fired to various maximum temperatures: (a) on MgO substrates and (b) Pt substrates.

approximation, $J_{c,m}=15\Delta M/d$, where d is the sample size of 2 mm. Figure 12 shows $J_{c,m}$ ($H_{app}=4$ T) for films fired on either Pt or on MgO as a function of the maximum firing temperature. The data show clearly the gradual increase of $J_{c,m}$ with firing temperature up to 4×10^4 A/cm^2 for the films fired on MgO. In contrast, the current density for those films fired on Pt at 1010 °C immediately increased to 3.5×10^4 A/cm^2 and improved only slightly to 4.5×10^4 A/cm^2 for films fired at higher temperatures.

IV. DISCUSSION

These results support previous work that bulk grain alignment in the Y-Ba-Cu-O system can be achieved by magnetically aligning Y123 crystallites in their normal state under ambient conditions, followed by partial melting of the powder compact and recrystallization of Y123 on unmelted oriented seeds.[21,22] The effect of alignment is readily apparent in the optical micrographs in Fig. 6, where the microstructures of the magnetically aligned samples show a distinct preferred orientation of grains compared to their nonaligned counterparts.

The magnetization data also show the effect of the magnetic alignment. The maximum anisotropy ratio for an aligned and densified sample obtained in this study was 2.6 for the film fired on Pt to a maximum temperature of 1010 °C. This compares well with a maximum anisotropy value of 2.9 achieved by Bourgault *et al.*[15] by melt processing in an applied field. However, it falls short of other reported results, notably a maximum anisotropy ratio of 5.45 reported by Ward *et al.*[11] for magnetically filter pressed and conventionally sintered material. The limiting ratio is 10, as determined by Dinger *et al.*[9] for single crystals, and was reproduced by Farrell *et al.*[10] for powdered single crystal material dispersed in an epoxy matrix and aligned in a magnetic field.

A key to achieving better texture in the fired material lies in improving the magnetic alignment procedure for the as-cast films. The P_{006} values determined for the as-cast magnetically aligned films in this study averaged 0.75 with anisotropy ratios on the order of 1.3. Using the same Y123 powder, but, by dispersing it in epoxy according to the procedure developed by Farrell *et al.*,[10] we have shown that P_{006} values of 0.98 can be achieved in the as-cast state with anisotropy ratios on the order of 2.9.[37] This latter value is higher than the best achieved in a fired sample in this work, so clearly the current fabrication procedure may be improved significantly.

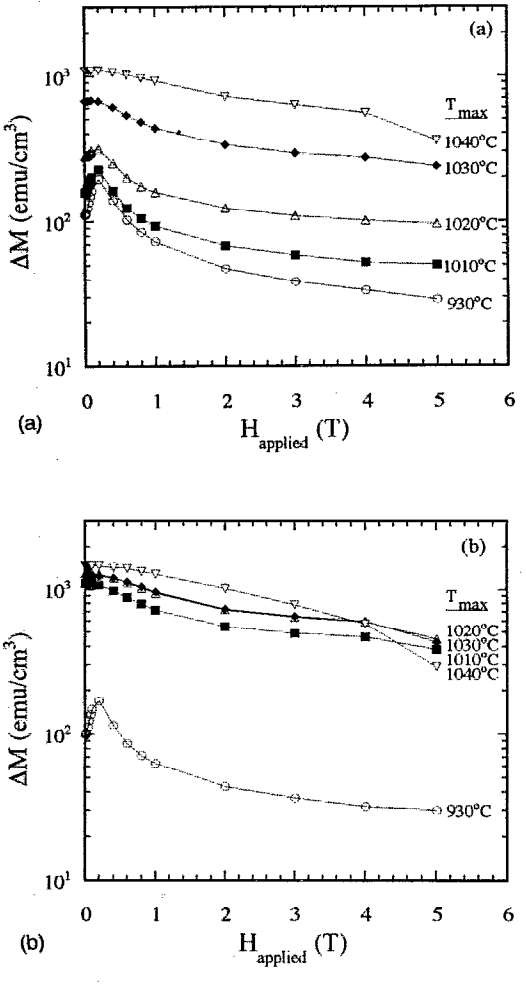

FIG. 11. ΔM as a function of applied field at 5 K for aligned Y123 films fired to various maximum temperatures on (a) MgO substrates and (b) Pt substrates.

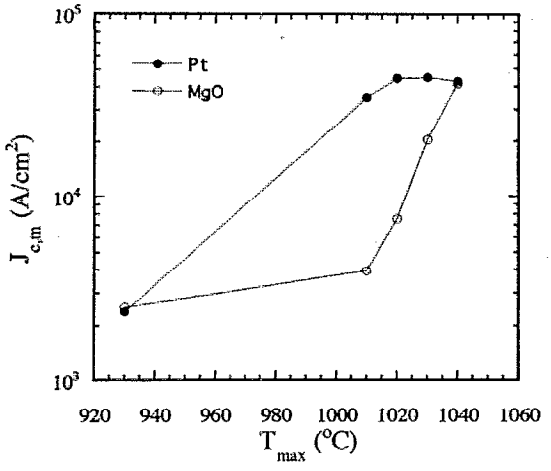

FIG. 12. Estimated critical current density ($H_{app}\|c$ axis at 5 K, 4 T) of aligned Y123 films as a function of maximum firing temperature.

The results also highlight the crucial role of the extent of Y123 melting during texture development in the magnetically aligned films. The purpose of the 2 h hold at 950 °C in the firing schedule shown in Fig. 1 is to allow a porous solid state sintered network of aligned powder particles to form. Since these films are densified in the absence of an applied field, it is necessary that some aligned Y123 crystallites remain unmelted and oriented to promote textured growth during recrystallization. When the extent of melting is controlled such that the network stays intact, an improvement in texture occurs as material recombines on the aligned nuclei, as shown in Fig. 6(b) for the film fired to 1010 °C on Pt. The presence of many unmelted nuclei accounts for the relatively fine microstructures observed. However, when complete or almost complete melting of the Y123 phase occurs, the few nuclei that form or remain are not preferentially oriented and the final microstructure consists of large, poorly aligned domains, as observed in the films fired to T_{max}=1040 °C shown in Fig. 7.

The results show clearly that the peritectic temperature and, consequently, the extent of melting are a strong function of the Pt content in the films. An approximately 70 °C reduction in T_p is observed in the DTA data for the Pt doped Y123 powder. Lewis *et al.*[22] have proposed a simple mechanism that explains the densification behavior in terms of this depression of T_p. No liquid is present below ~960 °C since the temperature is too low to activate the interaction between Pt and Y123. At ~960 °C the Pt substrate interacts with the Y123 film at contact points and peritectic liquid is formed at the film/substrate interface. As the temperature rises, more peritectic liquid containing Ba, Cu, and Pt is produced and redistributed throughout the film by capillary forces in the pore/grain boundary network. This hypothesis is supported by the SIMS data which shows a slightly higher Pt concentration at the grain boundaries than in the bulk of the grains. The redistribution of the Pt containing liquid facilitates local partial melting at particle surfaces throughout the Y123 film, leading to the high degree of densification and microstructural and chemical homogeneity, and superior superconducting properties observed in the films fired on Pt compared to those fired on MgO. Thus, the Pt-Y123 interaction opens a 70 °C window for partial melt processing in which the localized melting of Y123 greatly enhances the flexibility of this processing method. Without the Pt-Y123 interaction, complete melting of the Y123 film occurs within a few degrees above T_p, necessitating more precise temperature control, as demonstrated by the films fired on MgO.

Thus, this work represents a fundamental study of the processing of textured Y123 in the presence of platinum, and it suggests a host of new processing possibilities beyond exploiting simple film/substrate interactions. The incorporation of various concentrations of Pt directly into the Y123 films would allow precise tailoring of the extent of depressed localized melting, as evidenced by the DTA results. Furthermore, it is conceivable that this effect, combined with the depression of T_p induced by reducing the partial pressure of oxygen, will bring the melt processing window for Y123 down to temperatures where technologically relevant substrate materials such as silver (T_m=962 °C) could be utilized.

V. CONCLUSIONS

A detailed study of the effects of normal state magnetic alignment, thermal processing, and substrate interactions on the partial melt textured growth of Y123 thick films has been presented. Significant c-axis texture development and magnetization anisotropy ratios comparable with other magnetic alignment methods were observed in the fired films, especially in those fired on platinum substrates. Platinum was found to depress the peritectic temperature of pure Y123 by about 70 °C, opening up a much larger thermal processing window in which to fabricate high quality grain-aligned Y123 thick films. These results offer promise that, with additional research effort, technologically relevant bulk Y123 components may be produced.

ACKNOWLEDGMENTS

The authors wish to thank the following individuals for their assistance and/or permission to use of their equipment: Ray Strange (SQUID), Isaac Cherian and J. Bukowski (DTA), Dr. W. Klemperer (optical microscopy), K. Arndt, and M. Teepe. We also extend our thanks to the Center for Microanalysis of Materials, University of Illinois, supported by the U.S. Department of Energy under Contract No. DEFG02-91-ER45439, for access to XRD and SIMS equipment, and the School of Chemical Sciences Microanalytical Laboratory, University of Illinois, for performing the ICP analysis. This work has been supported by the National Science Foundation (NSF-DMR 91-20000) through the Science and Technology Center for Superconductivity.

[1] J. W. Ekin, A. I. Braginski, A. J. Panson, M. A. Janocko, D. W. Capone II, N. J. Zaluzec, B. Flandermeyer, O. F. de Lima, M. Hong, J. Kwo, and S. H. Liou, J. Appl. Phys. **62**, 4821 (1987).
[2] D. C. Larbalestier, D. Maeumling, X. Cai, J. Seuntjens, J. McKinnell, D. Hampshire, P. Lee, C. Meingast, T. Willis, H. Muller, R. D. Ray, R. G. Dillenburg, E. E. Hellstrom, and R. Joynt, J. Appl. Phys. **62**, 3308 (1987).
[3] S. Jin, R. C. Sherwood, T. H. Tiefel, R. B. van Dover, D. W. Johnson, and G. S. Grader, Appl. Phys. Lett. **51**, 855 (1987).

[4] S. Jin, T. H. Tiefel, R. C. Sherwood, M. E. Davies, R. B. van Dover, G. W. Kammlott, R. A. Fasnacht, and H. D. Keith, Appl. Phys. Lett. **52**, 2074 (1988).
[5] K. Salama, V. Selvamanickam, L. Gao, and K. Sun, Appl. Phys. Lett. **52**, 2352 (1989).
[6] M. Murakami, M. Morita, K. Doi, and K. Miyamoto, Jpn. J. Appl. Phys. **28**, 1189 (1989).
[7] P. J. McGinn, W. Chen, N. Shu, M. Lanagan, and U. Balachandran, Appl. Phys. Lett. **57**, 1455 (1990).
[8] M. J. Cima, M. C. Flemings, A. M. Figueredo, M. Nakade, H. Ishii, H. Brody, and J. S. Haggerty, J. Appl. Phys. **72**, 179 (1992).
[9] T. R. Dinger, T. K. Worthington, W. J. Gallagher, and R. L. Sandstrom, Phys. Rev. Lett. **58**, 2687 (1987).
[10] D. E. Farrell, B. S. Chandrasekhar, M. R. DeGuire, M. M. Fang, V. G. Kogan, J. R. Clem, and D. K. Finnemore, Phys. Rev. B **36**, 4025 (1987).
[11] P. J. Ward, P. F. Messer, E. A. Harris, and J. Crangle, Mater. Lett. **14**, 172 (1992).
[12] R. H. Arendt, A. R. Gaddipati, M. F. Garbauskas, E. L. Hall, H. R. Hart, Jr., K. W. Lay, J. D Livingston, F. E. Luborsky, and L. L. Schilling, *Proceedings of the Material Research Society Symposium* (Materials Research Society, Pittsburgh, PA, 1988), Vol. 99, p. 203.
[13] J. E. Tkaczyk and K. W. Lay, J. Mater. Res. **5**, 1368 (1990).
[14] A. Lusnikov, L. L. Miller, R. W. McCallum, S. Mitra, W. C. Lee, and D. C. Johnston, J. Appl. Phys. **65**, 3136 (1989).
[15] D. Bourgault, P. de Rango, R. M. Barbut, D. Braithwaite, M. R. Lees, P. Lejay, A. Sulpice, and R. Tournier, Physica C **194**, 171 (1992).
[16] N. Ogawa, I. Hirabayashi, and S. Tanaka, Physica C **177**, 101 (1991).
[17] M. Morita, M. Tanaka, S. Takebayashi, K. Kimura, K Miyamoto, and K. Sawano, Jpn. J. Appl. Phys **50**, L813 (1991).
[18] T. Izumi, Y. Nakamura, T. Sung, and Y. Shiohara, J. Mater. Res. **7**, 801 (1992).
[19] M. Yoshida, N. Ogawa, I. Hirabayashi, and S. Tanaka, Physica C **185**, 2409 (1991).
[20] G. W. Kammlott, T. H. Tiefel, and S. Jin, Appl. Phys. Lett. **56**, 2459 (1990).
[21] J. A. Lewis, T. Suratwala, and K. C. Arndt, IEE Trans. Appl. Superconductivity **3**, 1702 (1993).
[22] J. A. Lewis, M. R. Wegmann, C. E. Platt, and M. Teepe, Appl. Phys. Lett. **64**, 103 (1994).
[23] Seattle Specialty Ceramics, Woodinville, WA.
[24] Custom model, Cryomagnetics, Inc., Oak Ridge, TN.
[25] Model 55367 hinged tube furnace, Lindberg, Watertown, WI.
[26] Aldrich Chemical Co., Milwaukee, WI.
[27] Electronic Space Products International, Agoura, CA.
[28] Model PAD X, Scintag, Inc., Sunnyvale, CA.
[29] Model P2000, Perkin-Elmer Corp., Wilton, CT.
[30] Model BH2, Olympus, Lake Success, NY.
[31] Model IMS 5F, Cameca Instruments, Stamford, CT.
[32] Model MPMS, Quantum Design, San Diego, CA.
[33] Aldrich Chemical Co., Milwaukee, WI.
[34] Mallinckrodt, Inc., Paris, KY.
[35] Model 910 DSC with DTA cell, DuPont Instruments, Wilmington, DE.
[36] C. E. Platt and M. Teepe (unpublished work).
[37] J. A. Lewis, C. E. Platt, M. R. Wegmann, M. Teepe, J. L. Wagner, and D. G. Hinks, Phys. Rev. B Rapid Communications **48**, 7739 (1993).